Molecular Therapy
Original Article

Substrate Reduction Therapy for Sandhoff Disease through Inhibition of Glucosylceramide Synthase Activity

John Marshall,[1,2] Jennifer B. Nietupski,[1] Hyejung Park,[1] James Cao,[1] Dinesh S. Bangari,[1] Cristina Silvescu,[1,3] Terry Wilper,[1] Kristen Randall,[1] Drew Tietz,[1] Bing Wang,[1] Xiaoyou Ying,[1] John P. Leonard,[1,4] and Seng H. Cheng[1,5]

[1]Sanofi, 49 New York Avenue, Framingham, MA 01701, USA

Neuronopathic glycosphingolipidoses are a sub-group of lysosomal storage disorders for which there are presently no effective therapies. Here, we evaluated the potential of substrate reduction therapy (SRT) using an inhibitor of glucosylceramide synthase (GCS) to decrease the synthesis of glucosylceramide (GL1) and related glycosphingolipids. The substrates that accumulate in Sandhoff disease (e.g., ganglioside GM2 and its nonacylated derivative, lyso-GM2) are distal to the drug target, GCS. Treatment of Sandhoff mice with a GCS inhibitor that has demonstrated CNS access (Genz-682452) reduced the accumulation of GL1 and GM2, as well as a variety of disease-associated substrates in the liver and brain. Concomitant with these effects was a significant decrease in the expression of CD68 and glycoprotein non-metastatic melanoma B protein (Gpnmb) in the brain, indicating a reduction in microgliosis in the treated mice. Moreover, using *in vivo* imaging, we showed that the monocytic biomarker translocator protein (TSPO), which was elevated in Sandhoff mice, was normalized following Genz-682452 treatment. These positive effects translated in turn into a delay (~28 days) in loss of motor function and coordination, as measured by rotarod latency, and a significant increase in longevity (~17.5%). Together, these results support the development of SRT for the treatment of gangliosidoses, particularly in patients with residual enzyme activity.

INTRODUCTION

Sandhoff disease, a form of GM2 gangliosidosis, is caused by mutations in the *HEXB* gene, resulting in a deficiency in the activities of the enzymes β-hexosaminidase A and B. This deficiency results in the accumulation of a variety of substrates containing a β-linked terminal non-reducing N-acetyl glucosamine or N-acetyl galactosamine. These substrates include the glycosphingolipids GM2, GA2, and globoside; glycosaminoglycans (dermatan, chondroitin and keratan sulfates); and other oligosaccharides. The exact proportions of storage of these substrates in the lysosomal compartment is dependent upon the cell and tissue type.[1] In the CNS, the predominant substrates that accumulate are the glycosphingolipids GM2, GA2, and their nonacylated derivatives. It is presumed that this CNS accumulation of GM2 and GA2 is the primary cause of the pathophysiology because of their relative abundance and symptomatic similarities between the gangliosidoses.[2,3] Thus, a therapy targeted at reducing glycosphingolipid accumulation in the lysosomes may provide significant benefit for Sandhoff disease.

Patients with Sandhoff disease exhibit a spectrum of disease severity and are classified as infantile, juvenile, or adult variants, depending on age at onset. Currently, there are no approved therapies for Sandhoff disease beyond palliative and supportive care. Several therapeutic approaches have been proposed and evaluated in pre-clinical models, including gene therapy,[4,5] chaperone therapy,[6] hematopoietic stem cell or bone marrow transplantation,[7–9] enzyme-replacement therapy,[10,11] and substrate reduction therapy (SRT).[12–14] However, each potential therapy presents significant challenges before it can be developed into a successful treatment for patients. Gene therapy is an emerging technology with great potential, but for which there is currently no consensus on either the optimal viral vector type or mode of delivery for use in Sandhoff patients.[15,16] Despite ongoing clinical trials, there are as yet no reports of successful transplantation treatments in Sandhoff patients; this technique is also associated with significant morbidity.[17] Enzyme-replacement therapy, though effective in addressing the visceral disease, is unable to traverse the blood-brain barrier at therapeutic levels, and thus no neurological benefit has been observed.[18]

SRT is a clinically approved treatment paradigm for visceral manifestations of Gaucher disease.[19,20] The therapy seeks to reduce the

Received 7 February 2019; accepted 19 May 2019;
https://doi.org/10.1016/j.ymthe.2019.05.018.

[2]Present address: Moderna Therapeutics, 500 Technology Square, Cambridge, MA 02139, USA

[3]Present address: Bruker, Inc., 40 Manning Road, Manning Park, Billerica, MA 01821, USA

[4]Present address: CRISPR Therapeutics, 610 Main Street, Cambridge, MA 02139, USA

[5]Present address: Pfizer, Inc., 610 Main Street, Cambridge, MA 02139, USA

Correspondence: John Marshall, Sanofi, 49 New York Avenue, Framingham, MA 01701, USA.
E-mail: ramhoj@usa.net
Correspondence: Seng H. Cheng, PhD, Sanofi, 49 New York Avenue, Framingham, MA 01701, USA.
E-mail: seng.cheng@pfizer.com

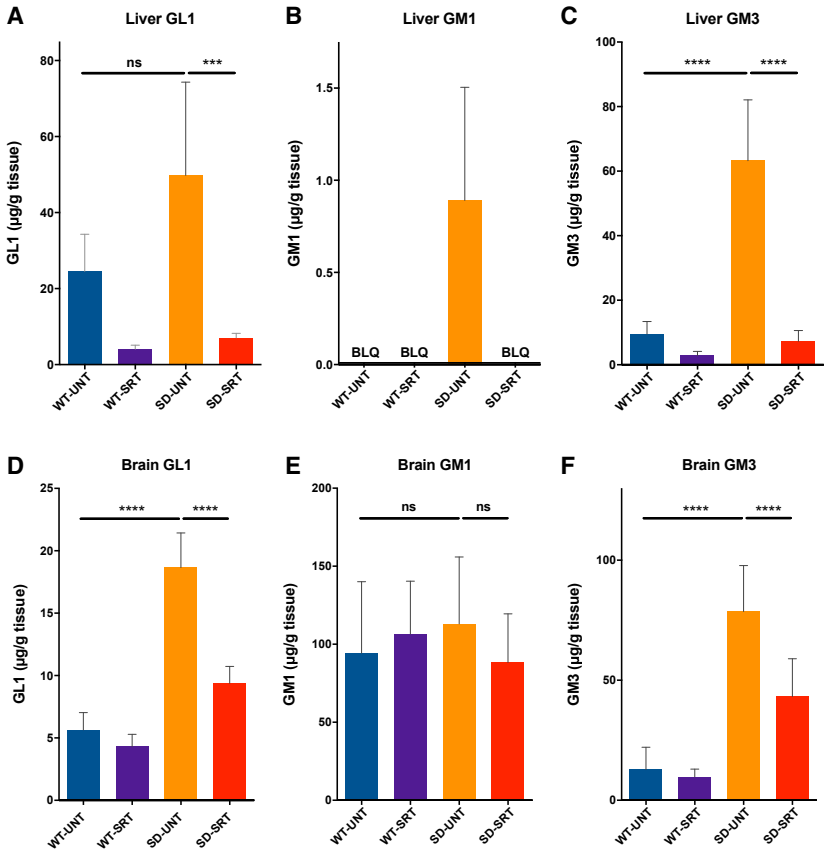

Figure 1. Genz-682452 Inhibits Glucosylceramide Synthase in Liver and Brain

Treatment with the GCS inhibitor Genz-682452 in *Hexb*$^{+/-}$ and *Hexb*$^{-/-}$ mice (WT-SRT and SD-SRT, respectively) from days 5 to 112 resulted in reductions of GL1 in liver (A) by ~85% and in brain (D) by ~50% relative to the corresponding untreated mice (WT-UNT and SD-UNT). GM1 (B) and GM3 (C) were also analyzed in liver and GM1 (E) and GM3 (F) in brain. GM1 levels were not affected by disease or treatment; however, GM3 levels mirrored the disease and treatment effects observed for GL1. BLQ, below the lower-level of quantitation. ***$p < 0.001$; ****$p < 0.0001$; ns, not significantly different. n = 6 per group. Error bars indicate SD.

amounts of lysosomal β-D-glucosylceramide (GL1) in Gaucher cells by inhibiting the enzyme (glucosylceramide synthase [GCS]) that is responsible for its synthesis. GL1 is the anabolic precursor of the glycosphingolipids that accumulate in Sandhoff disease (Figure S1). Thus, inhibition of this pathway in the CNS using a blood-brain-barrier-permeant inhibitor of the glycosphingolipid pathway may result in a reduced lipid burden. Preclinical studies using iminosugar-based inhibitors of GCS have been reported to provide significant survival benefit in the mouse model of Sandhoff disease.[12,21] However, the basis for these improvements remain unclear[14] and could include an off-target pathway unrelated to GCS inhibition.

The therapeutic potential of SRT has been demonstrated in other mouse models of lysosomal storage disorders (LSDs) with neuronopathic disease.[22,23] Here, we describe the use of a novel CNS-penetrant GCS inhibitor, Genz-682452,[23,24] to effect SRT of Sandhoff disease. Genz-682452 has been demonstrated to reduce glycosphingolipid biosynthesis in both visceral tissues and the CNS in preclinical models of related neuronopathic glycosphingolipidoses. The studies reported here were performed using a well-characterized mouse model that harbors a knockout of the *Hexb* gene[25] and has been used previously to evaluate other therapeutic modalities. The *Hexb*$^{-/-}$ mouse is a valid model of GM2 gangliosidosis, as it exhibits disease pathology, including substrate accumulation, neurodegeneration, and a shortened lifespan.[25]

Here, we report on the efficacy of daily administration of Genz-682452 at inhibiting the synthesis of glycosphingolipids and thereby the storage levels of related substrates in the tissues of Sandhoff mice. We show that GCS inhibition profoundly limited the accumulation of the glycosphingolipids GM2 and GA2, delayed the development of gliosis, and prolonged the longevity of these mice. The availability of an oral drug that can address CNS disease and some visceral manifestations could also offer an advantage over other approaches being considered, such as enzyme-replacement therapy and transplantation. As such, Genz-682452 may represent a solution, not only for Sandhoff disease, but also for the broader class of patients with glycosphingolipidoses, particularly in those with residual enzyme activity.

RESULTS

Genz-682452-Mediated Inhibition of GCS Lowers Liver and Brain Levels of Glycosphingolipids in Sandhoff Mice

SRT through inhibition of GCS has been shown to be effective at modulating disease progression in animal models of glycosphingolipidoses, such as Gaucher and Fabry disease. To determine if this therapeutic concept could be extended to include the GM2-gangliosidoses, we tested a small-molecule antagonist (Genz-682452) of GCS in a murine model of Sandhoff disease.[25]

Genz-682452 was administered to Sandhoff (*Hexb*$^{-/-}$) and healthy control (*Hexb*$^{+/-}$) mice, starting at 5 and ending on 112 days of age. Analysis of 112-day-old untreated Sandhoff mice (*Hexb*$^{-/-}$) showed that the GL1 levels in both the brain and liver were 2- to 3-fold higher than in the untreated healthy controls (Figures 1A and 1D). Treatment of *Hexb*$^{-/-}$ mice with Genz-682452 resulted in a reduction of GL1 levels in liver to ~15% of the levels in untreated *Hexb*$^{+/-}$ or *Hexb*$^{-/-}$ mice (Figure 1A). Levels of GL1 were also significantly lowered in Genz-682452-treated *Hexb*$^{-/-}$ mice, to ~50% of untreated levels (Figure 1D). That the brain GL1 levels were also

affected is consistent with the reported ability of Genz-682452 to access the CNS.

Whereas the Genz-682452-induced lowering of GL1 in both the liver and CNS compartments was expected, we also sought to determine if this translated to lowering of other lipids that were further downstream in the metabolic pathway. Moreover, as GL1 is not the primary lipid that accumulates in the lysosomes of patients with GM2 gangliosidoses, we also elected to measure the impact of GCS inhibition on the levels of GM1 and -3 (Figures 1B–1E). The levels of GM1 in the liver of $Hex^{+/-}$ mice (at 112 days of age) were below the level of quantitation (BLQ), but were slightly elevated in $Hexb^{-/-}$ mice (Figure 1B). Treatment of $Hexb^{-/-}$ mice with Genz-682452 lowered liver GM1 levels to BLQ. GM1 levels in the brain of untreated $Hexb^{-/-}$ and $Hex^{+/-}$ mice were not significantly different, and the levels were unaffected by treatment (Figure 1E).

In contrast, GM3, which typically accumulates to higher levels in patients with GM2 gangliosidoses, were determined to be elevated ~5-fold in the liver and brain of untreated $Hexb^{-/-}$ mice compared to $Hex^{+/-}$ mice (Figures 1C and 1F). $Hexb^{-/-}$ mice that were given Genz-682452, as noted above for GL1, showed significantly lower levels of GM3 in both liver and CNS, indicating that GCS antagonism could affect ganglioside levels downstream of the drug target. Similar reductions in GM1 and -3 levels were also noted in other visceral tissues assayed (e.g., spleen, lung, kidney, heart, and pancreas) following treatment (Figure S2). Hence, SRT with Genz-682452 was effective at lowering the pathogenic lipids shown to be associated with the development of GM2-gangliosidoses.

A complex array of specific substrates of hexosaminidases A and B that contain a terminal non-reducing N-acetylhexosamine in β-linkage also accumulated in the lysosomes of cells from Sandhoff disease patients. These include oligosaccharides, glycosaminoglycans, glycoproteins, and glycosphingolipids in various amounts and proportions, depending on the source of the cell or tissue. To determine if these entities were similarly reduced by SRT with Genz-682452, we measured the levels of the glycosphingolipids GM2, GA2, and GL4 and the glycosaminoglycan dermatan sulfate (Figure 2). Analysis of 112-day-old $Hexb^{-/-}$ mice (SD-SRT) given Genz-682452 showed significantly lower levels of GM2 in liver (Figure 2A), other visceral tissues (Figure S2), and brain (Figure 2E), relative to untreated $Hexb^{-/-}$ mice (SD-UNT). Similar results were also noted for GA2 (Figures 2B and 2G), GL4 (Figures 2C and 2H), and lyso-GM2 in the brain (Figure 2F). All the glycosphingolipids in the Genz-682452-treated $Hexb^{-/-}$ mice were reduced by ~85% in liver and by ~50% in brain tissue. No significant changes were observed in the brains of SRT-treated $Hexb^{+/-}$ mice (wild-type [WT]-SRT) relative to untreated. Hence, Genz-682452 treatment resulted in significantly lower levels of disease-relevant glycosphingolipids in the visceral tissues and brain of Sandhoff mice.

Dermatan sulfate is a glycosaminoglycan and a non-glycosphingolipid substrate of hexosaminidase that was found to be elevated ~10-fold in liver of 112-day-old Sandhoff mice compared to their phenotypic WT controls (Figure 2D). As expected, treatment of $Hexb^{-/-}$ mice with Genz-682452 did not alter the liver levels of this glycosaminoglycan, as it is unrelated to the glycosphingolipid pathway.

Genz-682452 Mediates Lowering of GM2 Levels in Broad Regions of Brain of Sandhoff Mice

To further evaluate the efficacy of Genz-682452 in the brain, unfixed, flash-frozen, sagittal sections (10 μm) were generated from 112-day-old $Hexb^{-/-}$ and $Hexb^{+/-}$ mice. The sections were processed for tissue mass spectrometry imaging (tMSI) and analyzed for the relative abundance of the C_{18} acyl chain isoform of GM2 (specifically, GM2 *m/z* 1,382.7 GalNAcβ1-4[NeuAcα2-3]Galβ1-4Glcβ-Cer[d18:1/18:0]). Tissue sections from $Hexb^{+/-}$ mice that were untreated or treated with Genz-682452 (WT-UNT and WT-SRT, respectively) showed, as expected, no detectable signals for GM2 (Figure 3). In contrast, untreated $Hexb^{-/-}$ mice (SD-UNT) showed high levels of GM2 throughout the brain, including in the cerebellum folia, midbrain, hypothalamus, basal forebrain, caudate, ventral striatum, hippocampus, and olfactory bulb (Figure 3). Supporting these tMSI data, histopathological analysis of these same sections showed evidence of vacuolated neurons laden with lipid deposits (D.S.B., unpublished data). Importantly, tMSI of Genz-682452 treated $Hexb^{-/-}$ mice brains (SD-SRT) showed that SRT decreased the extent of C_{18}-GM2 accumulation throughout the brain by approximately 2-fold compared with untreated $Hexb^{-/-}$ mice (Figure 3). Hence, the data corroborate the quantitation data for brain glycosphingolipid levels, using MS, as reported in Figure 2.

Genz-682452 Significantly Reduces the Extent of Gliosis in Brain of Sandhoff Mice

Brain tissues from 112-day-old $Hexb^{-/-}$ and $Hexb^{+/-}$ mice were also analyzed for evidence of inflammation by measuring the mRNA levels (using RT-PCR) of the biomarkers CD68 (for microglia), glycoprotein non-metastatic melanoma B protein (Gpnmb; for neuroinflammation), and glial fibrillary acidic protein (GFAP; for activated astrocytes). Levels of these biomarkers were low and remained unchanged in $Hexb^{+/-}$ mice that had been treated or not treated with Genz-682452 (Figure 4). However, brain tissue from $Hexb^{-/-}$ mice showed significantly elevated levels of CD68, Gpnmb, and GFAP mRNA relative to $Hexb^{+/-}$ mice, indicating a heightened level of gliosis. Treatment of $Hexb^{-/-}$ mice with Genz-682452 significantly lowered the levels of these biomarkers of gliosis, albeit not to normal levels.

Brain sections were further evaluated by immunohistochemistry (IHC) using an anti-Gpnmb antibody (Figure 4D). Sections from the thalamus and brainstem exhibited negligible positive staining for Gpnmb in $Hexb^{+/-}$ mice (WT-UNT), whereas those from $Hexb^{-/-}$ mice showed a high degree of immunopositivity (SD-UNT); microscopic evaluation indicated that the majority of these were microglia. Treatment of the $Hexb^{-/-}$ mice with Genz-682452 reduced the extent of Gpnmb staining in these sections (SD-SRT).

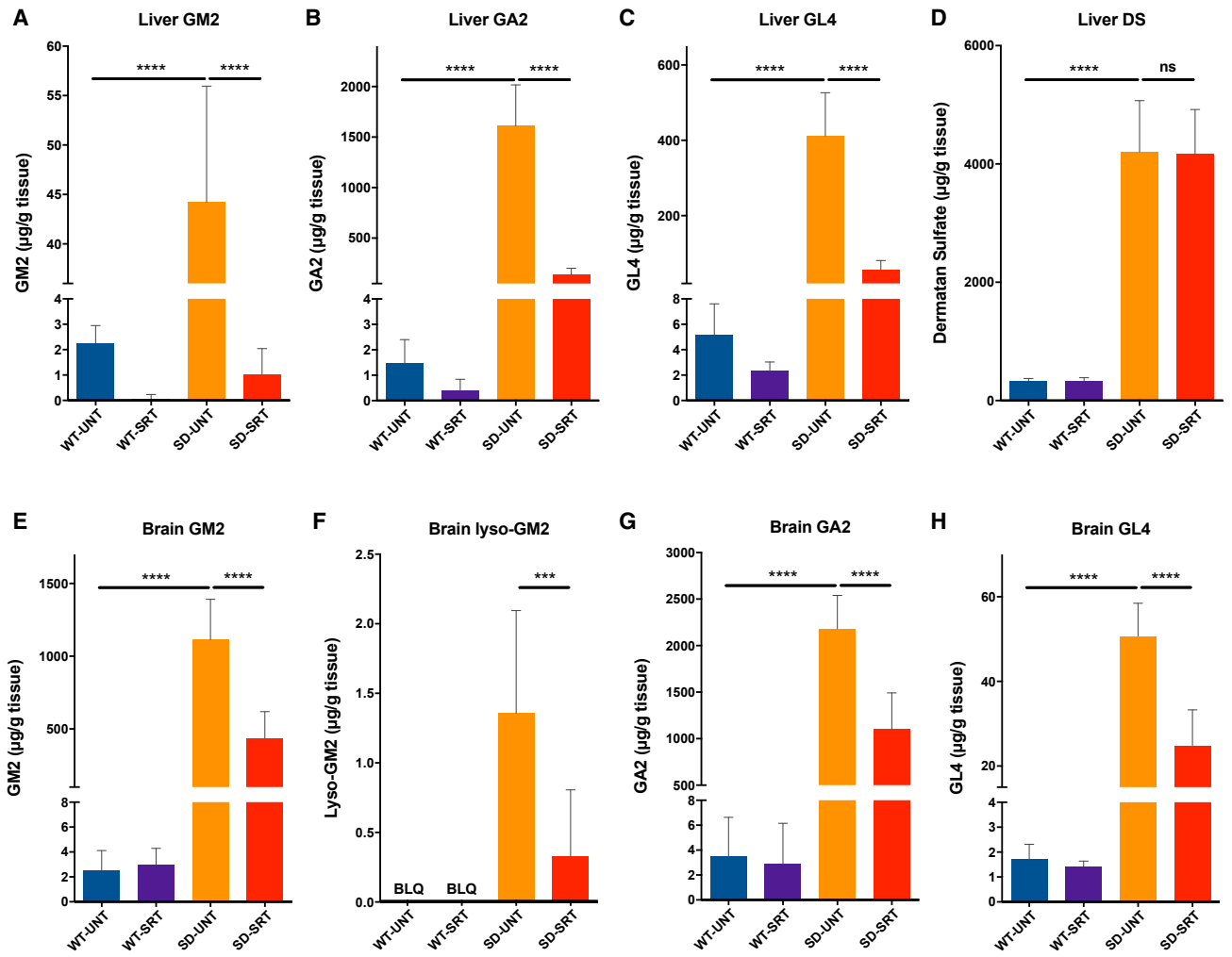

Figure 2. Genz-682452 Significantly Inhibits Accumulation of Substrates of β-Hexosaminidase A and B

Treatment of mice with the GCS inhibitor Genz-682452 in *Hexb*$^{+/-}$ and *Hexb*$^{-/-}$ mice (WT-SRT and SD-SRT, respectively) from days 5 to 112 resulted in significant reductions in the levels of glycosphingolipids that accumulate in Sandhoff disease. Liver levels of GM2 (A), GA2 (B), and GL4 (C) in Genz-682452-treated *Hexb*$^{-/-}$ mice (SD-SRT) were all reduced by ~85%, relative to the corresponding untreated mice (SD-UNT). Brain levels of GM2 (E), lyso-GM2 (F), GA2 (G), and GL4 (H) in Genz-682452-treated *Hexb*$^{-/-}$ mice (SD-SRT) were all reduced by at least 50%, relative to corresponding untreated mice (SD-UNT). Dermatan sulfate (D), which is a glycosaminoglycan substrate of β-hexosaminidase, was significantly elevated in liver of *Hexb*$^{-/-}$ mice and, as expected, was unaffected by treatment with Genz-682452. BLQ, below the lower-level of quantitation. ***p < 0.001; ****p < 0.0001; ns, not significantly different. n = 6 per group. Error bars indicate SD.

Quantitation of the areas in the thalamus that stained positively for Gpnmb (Figure 4E) revealed a significant reduction in signal in *Hexb*$^{-/-}$ mice treated with Genz-682452 (SD-SRT) compared to untreated *Hexb*$^{-/-}$ mice (SD-UNT). In the brainstem, a trend toward reduced Gpnmb immunopositivity was also noted in Genz-682452-treated *Hexb*$^{-/-}$ mice, but the magnitude of change did not reach statistical significance.

In Vivo Brain Imaging of a Fluorescent TSPO Ligand in Sandhoff Mice as a Potential Translational Biomarker of Efficacy

The 18 kDa translocator protein (TSPO), which forms part of the mitochondrial permeability transition pore, is highly expressed in activated microglia.[26] Here, we used a near-infrared TSPO ligand (VUIIS-1520) to determine if TSPO could function as a potential non-invasive translational biomarker of efficacy following SRT of Sandhoff mice. Mice were injected intravenously with VUIIS-1520 at 1, 2, 3, and 4 months of age, and the animals were imaged with the IVIS SpectrumCT *in vivo* imaging system, 24 h after the injection. At the end of the study (approximately 4-month-old mice), organs were also removed and imaged to determine qualitative differences between *Hexb*$^{+/-}$ and *Hexb*$^{-/-}$ mice (Figure 5A). An elevated TSPO-ligand signal (indicated by intense yellow) was observed in all tissues of untreated *Hexb*$^{-/-}$ mice (SD-UNT) but especially brain, liver, and kidney. Organs from *Hexb*$^{-/-}$ mice treated

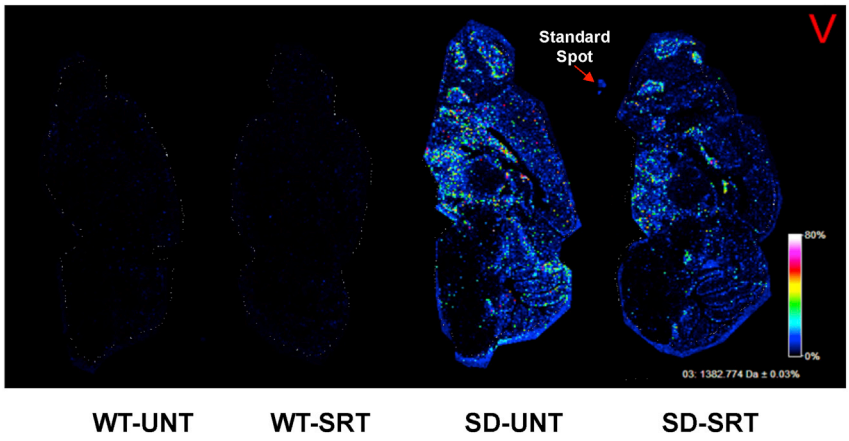

Figure 3. Tissue Mass Spectrometry Imaging of Sagittal Brain Sections for GM2 Levels

Mice were treated with the GCS inhibitor Genz-682452 in *Hexb*$^{+/-}$ and *Hexb*$^{-/-}$ mice (WT-SRT and SD-SRT, respectively) from days 5 to 112 and compared to corresponding untreated mice (WT-UNT and SD-UNT, respectively). At day 112, mice were euthanized, and sagittal brain sections (10 μm) were taken for tissue mass spectrometry imaging to probe for the relative abundance of C_{18}-GM2. Images were acquired at 35 μm spatial resolution using Autoflex MALDI TOF/TOF and were normalized with the root mean square (RMS) algorithm (denoted by the red V). Images are representative of brain sections from two animals per experimental group (n = 2). GM2 was barely detectable in brain sections from *Hexb*$^{+/-}$ mice that were untreated or treated with Genz-682452 (WT-UNT and WT-SRT, respectively). However, untreated *Hexb*$^{-/-}$ mice showed relatively high levels of GM2 in many regions of the brain, notably the cerebellum folia, midbrain, hypothalamus, basal forebrain, caudate, ventral striatum, hippocampus, and olfactory bulb. *Hexb*$^{-/-}$ mice treated with Genz-682452 (SD-SRT) revealed an approximately 2-fold decreased level of C_{18}-GM2 throughout the brain in comparison to the untreated mice (SD-UNT).

with Genz-682452 (SD-SRT) showed a TSPO probe signal that was markedly lower and akin to those from *Hexb*$^{+/-}$ mice (WT-UNT).

Results of the direct *in vivo* imaging studies performed at the 1, 2, 3, and 4 month time points are shown in Figure 5B. The fluorescence intensity of TSPO noted in *Hexb*$^{-/-}$ mice was similar to *Hexb*$^{+/-}$ mice at the early time points (1 and 2 months) indicating that, at this early age, the level of microgliosis in *Hexb*$^{-/-}$ mice was low, as reported previously.[14] However, by 3 and 4 months of age, the fluorescence intensity in the untreated *Hexb*$^{-/-}$ mice was 2- to 3-fold higher than in the untreated *Hexb*$^{+/-}$ mice. Consistent with the measurements reported above, *Hexb*$^{-/-}$ mice treated with Genz-682452 showed no increase in fluorescence intensity beyond that noted for *Hexb*$^{+/-}$ mice. This normalization of TSPO-probe signal in the Genz-682452-treated *Hexb*$^{-/-}$ mice provides additional evidence that gliosis was attenuated by this therapeutic approach.

Sandhoff Mice Treated with Genz-682452 Show Improved Motor Function and Greater Longevity

We measured phenotypic and behavioral changes of *Hexb*$^{-/-}$ mice to determine if treatment with Genz-682452 affects disease progression and confers a therapeutic effect. Body weights of the mice were recorded throughout the study period to ascertain the tolerability of Genz-682452 (toxicity) and to monitor the impact of disease advancement. As shown in Figure 6A, no significant difference in the weight of both male and female mice was observed between either *Hexb*$^{-/-}$ and *Hexb*$^{+/-}$ mice before disease onset, at 15 weeks of age; the weights were also similar between untreated or Genz-682452-treated animals during this period. However, in contrast to *Hexb*$^{+/-}$ mice, both male and female *Hexb*$^{-/-}$ mice showed a progressive loss in body weight after 15 weeks of age, irrespective of treatment.

Neuromuscular coordination as determined, using the rotarod test as an indicator of neurodegeneration (Figure 6B). At the first collection time point (day 84), a significant deficit in rotarod latency (~100 s) was already evident in the untreated *Hexb*$^{-/-}$ mouse group (SD-UNT), whereas the latency to fall of the Genz-682452-treated *Hexb*$^{-/-}$ cohort (SD-SRT) was not significantly different from the WT-SRT or WT-UNT group (~200 s). At the second time point (day 98), SD-UNT mice exhibited a further decline in performance (latency of ~41 s); by contrast, that of the SD-SRT cohort remained the same as the WT-SRT controls. However, at day 112, the SD-SRT animals showed a significant decline in performance relative to the healthy controls, suggesting that treatment with Genz-682452 had delayed the onset (by ~28 days) and subsequent progression of disease. Genz-682452 treatment had no effect on the rotarod performance of the *Hexb*$^{+/-}$ mice, relative to the untreated cohort. In this assay, there were no differences in rotarod performance between male and female mice.

All *Hexb*$^{-/-}$ mice were also evaluated daily starting at 100 days of age for their ability to right themselves upon being placed in a supine position. If the elapsed time for a mouse to right itself was >30 s, the mouse was euthanized according to institutional guidelines, and the day was recorded as its survival time (Figure 6C). Using this criterion, untreated *Hexb*$^{-/-}$ mice (SD-UNT) had a median survival of 134 days; by contrast, Genz-682452-treated *Hexb*$^{-/-}$ mice (SD-SRT) had an extended median survival of 157.5 days. This represented an increased longevity of 23.5 days or 17.5%, which mirrored the difference in rotarod performance described above. No apparent difference in survival was noted between treated and untreated male and female *Hexb*$^{-/-}$ mice. No deaths were recorded in the groups of *Hexb*$^{+/-}$ mice over the study time frame.

DISCUSSION

SRT as a therapeutic modality has demonstrated utility in several animal models of LSDs[27] and is an approved first-line clinical intervention for patients with type 1 Gaucher disease.[28,29] Current clinically approved SRT drugs are inhibitors of GCS, the initial enzyme involved in glucosphingolipid biosynthesis. Here, we continued to

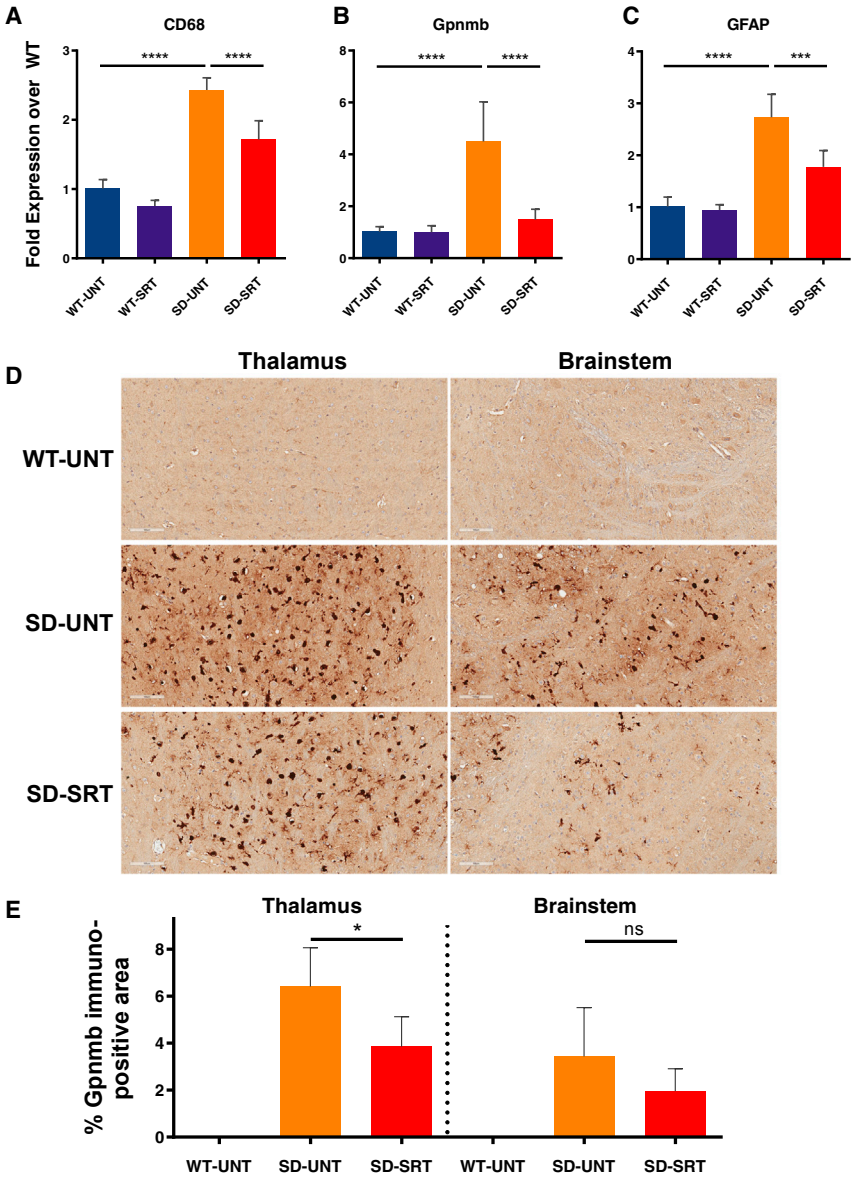

Figure 4. Genz-682452 Treatment Attenuates mRNA Levels of Inflammatory Markers and Reduces Immunohistochemical Signals of Brain Gliosis in *Hexb*$^{-/-}$ Mice

Brain tissue of *Hexb*$^{+/-}$ and *Hexb*$^{-/-}$ mice (WT-SRT and SD-SRT, respectively) treated with the GCS inhibitor Genz-682452 from days 5 to 112 was processed for mRNA quantitation by RT-PCR and compared to corresponding untreated mice (WT-UNT and SD-UNT, respectively). The biomarkers evaluated were CD68 for microglia (A), glycoprotein non-metastatic melanoma B (Gpnmb) for neuroinflammation (B), and glial fibrillary acidic protein (GFAP) for activated astrocytes (C). Genz-682452 treatment in *Hexb*$^{+/-}$ mice had no effect on relative levels of the mRNA for these biomarkers (WT-SRT versus WT-UNT). *Hexb*$^{-/-}$ mice had significantly more CD68, Gpnmb, and GFAP mRNA than WT mice, indicating elevated levels of gliosis. Genz-682452 treatment resulted in a significant reduction in the levels of mRNA of all three biomarkers of gliosis. (D) Immunohistochemical staining of brain sections with an anti-Gpnmb antibody revealed significant immunopositive staining in many regions. Illustrative sections from thalamus and brainstem showing elevated Gpnmb signal in cell types of microglial morphology are shown. (E) Quantitation of the areas staining positive for Gpnmb confirmed that elevated levels were present in untreated *Hexb*$^{-/-}$ mice (SD-UNT), and the signal was reduced when treated with Genz-682452 (SD-SRT). *$p < 0.05$; ***$p < 0.001$; ****$p < 0.0001$; ns, not significantly different. n = 6 per group. Error bars indicate SD.

investigate the potential of a novel GCS inhibitor, Genz-682452, which we previously showed is efficacious in addressing disease manifestations in murine models of Fabry disease[24] and neuronopathic Gaucher disease.[23] However, as GCS catalyzes the first step in the biosynthesis of glucosphingolipids, we sought to investigate whether this concept could be applied to address the gangliosidoses (Tay-Sachs, Sandhoff, GM2 activator protein deficiency, and GM1 gangliosidosis), as well. The experiments described herein were designed to demonstrate the potential benefit of SRT for Sandhoff disease and to identify prospective translational parameters.

Daily administration of Genz-682452 for 6 months was well tolerated by the *Hexb*$^{+/-}$ mice. There were no observed effects on their body weights, daily clinical observations, or histological changes following necropsy. Genz-682452-treated Sandhoff mice exhibited a delay in displaying deficits on the rotarod test and, importantly, a significantly improved survival benefit, despite there being no residual enzyme activity in this model. These observations were akin to what we had reported previously using this GCS inhibitor in other LSD mouse models.[23,24] As expected, treatment with Genz-682452 reduced the levels of GL1 and related glycosphingolipids in most tissues, including the brain (Figures 1, 2, and S2). The reductions in levels of GM3 following treatment with Genz-682452 recapitulated those of GL1, suggesting that GCS is the rate-limiting enzyme in the glucosphingolipid pathway in the brain. The glycosphingolipids specifically associated with Sandhoff disease (GM2, GA2, GL4, and lyso-GM2) were all highly elevated in the *Hexb*$^{-/-}$ mice relative to the *Hexb*$^{+/-}$ mice, including in brain tissue, where the gangliosides were 500-fold above normal levels. Treatment of *Hexb*$^{-/-}$ mice with Genz-682452 reduced the substrate levels by approximately 50% and increased lifespan by 17.5%, when compared to untreated controls. Interestingly, offspring from a genetic cross of *Hexb*$^{-/-}$ with *GalNAcT*$^{+/-}$ mice that showed ~50% less GM2 and GA2 than *Hexb*$^{-/-}$ animals also exhibited an increased lifespan of 18%.[30] We can speculate that, in a mouse model with residual β-hexosaminidase activity, we could expect the benefit of SRT to be

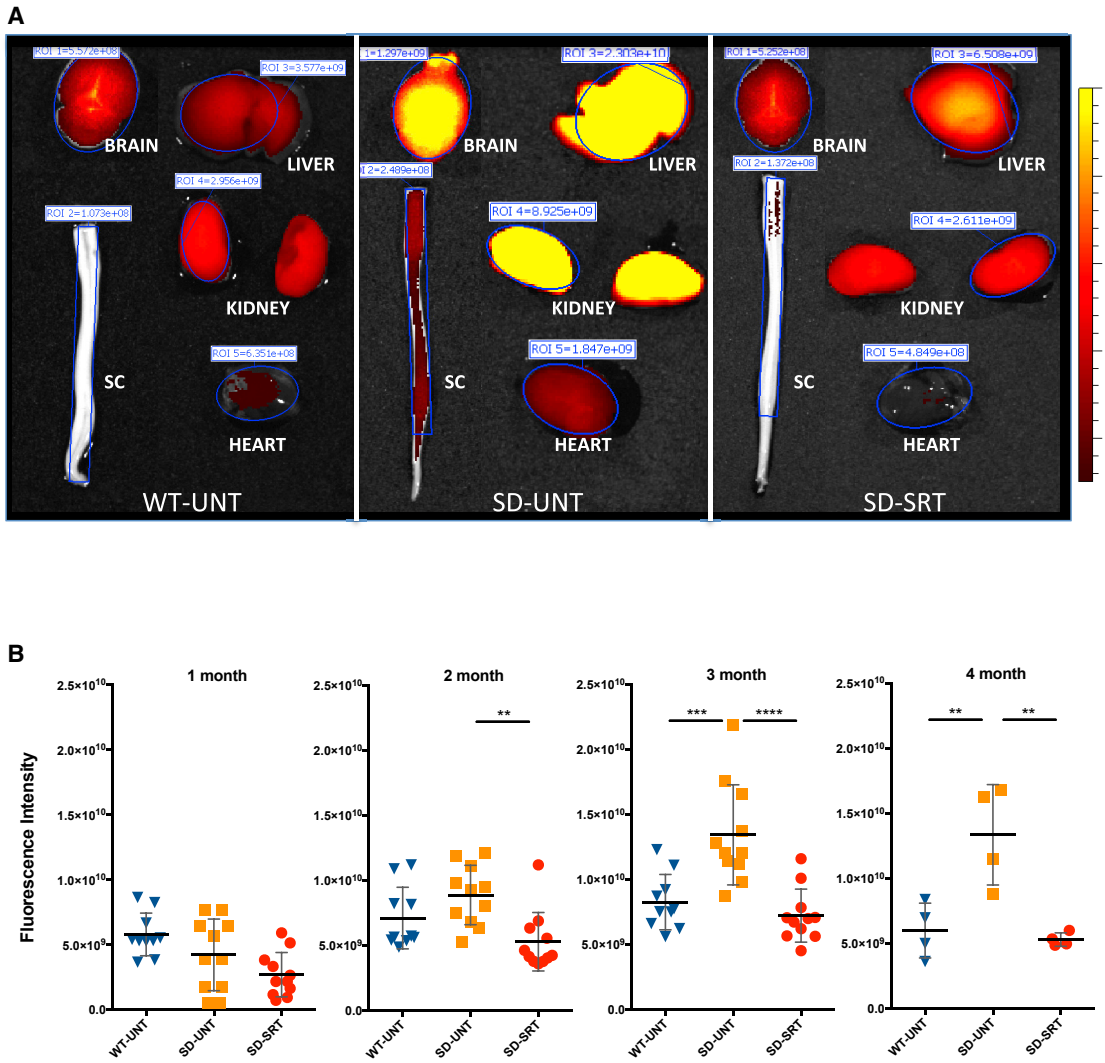

Figure 5. Increased TSPO Fluorescent Ligand Signal in *Hexb*$^{-/-}$ Mice Is Attenuated by Genz-682452 Treatment

A near infrared fluorescent ligand (VUIIS-1520) that binds to TSPO showed that the inflammatory biomarker was upregulated in Sandhoff mice. (A) Signal intensities of the ligand in isolated brain, liver, spinal cord (SC), kidney, and heart are shown at 113 days of age. All tissues, particularly the brain and liver of untreated *Hexb*$^{-/-}$ mice (SD-UNT), exhibited a high signal that diminished in intensity following treatment with Genz-682452 (SD-SRT). Treated *Hexb*$^{-/-}$ mice exhibited a TSPO-ligand intensity similar to that of untreated *Hexb*$^{+/-}$ mice (WT-UNT). (B) Longitudinal quantitation of *in vivo* TSPO-ligand fluorescence intensity demonstrated an increasing signal strength in untreated *Hexb*$^{-/-}$ mice (SD-UNT) with time. Fluorescence intensity in untreated *Hexb*$^{+/-}$ (WT-UNT) and Genz-682452-treated *Hexb*$^{-/-}$ mice remained unchanged throughout the study, indicating that SRT was effective in reducing inflammation in *Hexb*$^{-/-}$ mice. **p < 0.01; ***p < 0.001; ****p < 0.0001. Error bars indicate SD.

greater. These findings also support the notion that the accumulation of brain ganglioside is primarily responsible for the shortened lifespan of Sandhoff mice, rather than other substrates of β-hexosaminidase.

The relative abundance of GM2 and GA2 glycosphingolipids in *Hexb*$^{+/-}$ mice are similar in both liver and brain (Figure 1). However, in *Hexb*$^{-/-}$ mice, there was significantly more GA2 relative to GM2, especially in the liver, where a 10-fold excess of GA2 was detected. This is reportedly due to the presence of the sialidases *Neu3* and *Neu4* that are active in mice,[31,32] but not in humans. These sialidases provide a bypass degradative pathway for GM2 that, in the mouse model of Tay-Sachs disease (another GM2 gangliosidosis), was thought to limit the observed pathology.[33]

The role of lysosphingolipids in the pathogenicity of LSDs has been widely discussed, with the consensus being that, for most diseases, they play an important role in development of sequelae and can therefore serve as useful biomarkers of therapeutic efficacy.[34–38] It has been shown that lysosphingolipids are generated in the lysosome by the action of acid ceramidase on the accumulated glycosphingolipid.[39] One such member, lyso-GM2, has been identified as an important biomarker of Sandhoff disease in the CNS of both mouse models[40]

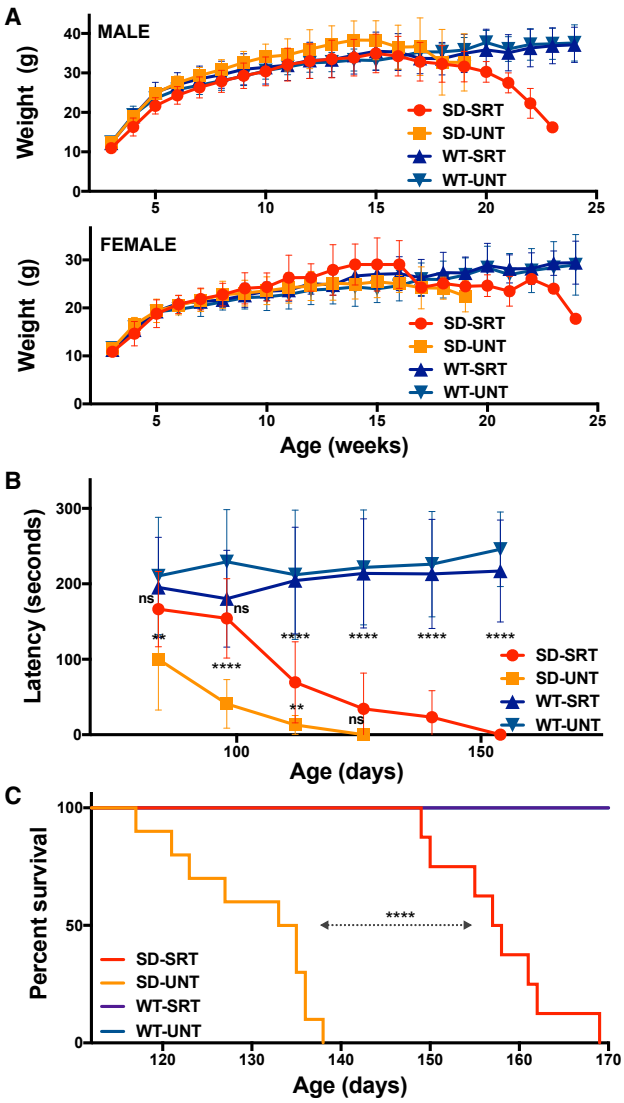

Figure 6. Genz-682452 Treatment Delays Development of Rotarod Deficits and Increases Longevity of *Hexb*$^{-/-}$ Mice

(A) Mice were weighed weekly throughout the study as a measure of their general health. The body weights of male and female mice are plotted separately. There was no significant difference in body weights between *Hexb*$^{+/-}$ (WT) and *Hexb*$^{-/-}$ mice (SD) or between untreated (UNT) and Genz-682452-treated animals (SRT) through 15 weeks of age. Thereafter, body weights of *Hexb*$^{-/-}$ mice began to drop as disease symptoms progressed. (B) Mice were evaluated on an accelerating rotarod assay to measure the progressive deficits in hind limb function. By 84 days of age, untreated *Hexb*$^{-/-}$ mice (SD-UNT) exhibited a significant decrease in latency that deteriorated over time. Treatment with Genz-682452 (SD-SRT) delayed the onset and progression of the rotarod deficit in *Hexb*$^{-/-}$ mice by approximately 4 weeks. (C) *Hexb*$^{-/-}$ mice were evaluated daily from 100 days of age for their ability to right themselves from supine. If the time taken was >30 s the mouse was euthanized to minimize unnecessary suffering. According to this criterion, untreated *Hexb*$^{-/-}$ mice (SD-UNT) had a median survival of 134 days. Genz-682452-treated *Hexb*$^{-/-}$ mice (SD-SRT) had extended median survival of 157.5 days and increased longevity of 17.5%. **p < 0.01; ****p < 0.0001; ns, not significantly different. N = 8-10 per group. Error bars indicate SD.

and patients.[41] Here, we demonstrated that Genz-682452-mediated SRT led to an approximately 50% reduction in brain GM2 and a concomitant 75% decrease in lyso-GM2 levels. The significant reduction of this potentially neuroinflammatory lipid was an important objective of these studies and supports the use of SRT in patients.

Hexb$^{-/-}$ mice and Sandhoff patients develop extensive and progressive microgliosis that is a likely cause of the noted neurodegeneration.[42–45] Treatment of the *Hexb*$^{-/-}$ mice with Genz-682452 resulted in reduced ganglioside storage and a concomitant reduction in biomarkers of brain gliosis. Microglial (CD68) and astrocytic (GFAP) markers that were both significantly elevated in all brain regions at the beginning of the study were significantly reduced by SRT. Two other markers of microglial activation, Gpnmb and TSPO, were also responsive to the effects of Genz-682452 treatment. Gpnmb is emerging as a useful biomarker of neuroinflammation in neuronopathic diseases.[46–48] TSPO has also been shown to be a viable marker of activated microglia[26,49] through positron emission tomographic (PET) imaging using TSPO-binding probes.[50,51] An elevated brain TSPO probe signal has previously been reported in the *Hexb*$^{-/-}$ mouse.[52] Here, we demonstrated normalization of the TSPO probe signal in live *Hexb*$^{-/-}$ mice treated with Genz-682452, thus validating a potential translational biomarker for tracking efficacy of SRT in patients. It has been reported that some TSPO ligands can provide neuroprotection[53] and therefore may affect disease progression. However, the infrequent doses of VUIIS-1520 in this study (one dose per month for 4 months) did not affect the animals' phenotype, histopathology, or tissue substrate levels when compared to mice that had not been subjected to TSPO imaging.

The non-sphingolipid substrates of β-hexosaminidase, such as glycosaminoglycans, were not affected by GCS inhibition, as demonstrated by the unchanged liver levels of dermatan sulfate in Genz-682452-treated *Hexb*$^{-/-}$ mice. These other substrates, which reportedly are not a major driver of brain pathology,[2,3] may require a secondary intervention, such as intravenous enzyme-replacement infusions or liver-directed gene therapy. However, the major cause of morbidity in Sandhoff patients is their CNS disease, which is difficult to treat without highly invasive procedures. Thus, the use of a brain-penetrant, small-molecule inhibitor of brain gangliosides should provide the greatest benefit with the least challenging delivery paradigm.

In summary, these data describe the successful use of a specific inhibitor of GCS, Genz-682452, to delay the progression of Sandhoff disease. The approval of eliglustat for SRT for type 1 Gaucher disease provides support for using a similar approach for treating the related glycosphingolipidoses. Importantly, by using a CNS-accessible GCS inhibitor, the concept can be extended to address neuronopathic disease. However, measuring clinical outcome in LSD patients remains challenging, due to the variability of symptoms, rate of disease progression, and relative paucity of patients. Additionally, neuronopathic LSDs exhibit irreversible neurodegenerative changes, and there are few validated CNS-related biomarkers to monitor efficacy of

treatment.[54] Here, we demonstrated that several biomarkers of neurodegenerative disease—namely, Gpnmb,[47] glycosphingolipid substrates,[55,56] and TSPO[50,51]—were readily detected in the mouse model of Sandhoff disease and were normalized with SRT. Finally, these data, describing the successful use of Genz-682452 in Sandhoff mice support its further development for the treatment of this disease and, potentially, other related gangliosidoses, particularly in patients with residual enzyme activity.

MATERIALS AND METHODS

Animal Studies

All animal experiments were performed in a facility accredited according to Association for Assessment and Accreditation of Laboratory Animal Care (AAALAC) standards, using protocols approved by the Institutional Animal Care and Use Committee (IACUC) of Sanofi.

The *Hexb*$^{-/-}$ mouse,[25] which is deficient in β-hexosaminidase subunit β, was used under license from the NIH and obtained from The Jackson Laboratory (Bar Harbor, ME, USA). Breeding to generate mice used in the studies reported here was between *Hexb*$^{-/-}$ males (8–12 weeks old) and *Hexb*$^{+/-}$ females (13–16 weeks old). Genotyping was performed on tail clips from 1-day post-natal (p1) pups, to identify homozygous *Hexb*$^{-/-}$ (Sandhoff, SD) and heterozygous *Hexb*$^{+/-}$ (phenotypic WT) mice. The *Hexb*$^{+/-}$ mice present as phenotypic WT, as previously reported[25] and were used as control mice for these studies. SRT in the mice was induced with a GCS inhibitor, Genz-682452, and was initiated in the mice at 5 days of age. Genz-682452 was administered to pre-weaned mice via daily intraperitoneal (i.p.) injections (12.5 mg/kg/day), and after weaning (from day 21), was administered as a component of a pelleted diet (modified 5053 rodent diet; TestDiet, Richmond, IN, USA) to a dose of ~60 mg/kg/day. A cohort of mice was treated until they were 112 days old, when tissues were taken for various analyses. A second cohort was exclusively used for a longitudinal study to evaluate a fluorescent translocator protein (TSPO) probe as a translational biomarker in the brains of the mice. A third group of mice was used for a longitudinal rotarod study and to test the effects of SRT on survival. *Hexb*$^{-/-}$ mice develop neurodegenerative disease and exhibit difficulties in drinking, feeding, and grooming from about 14 weeks of age. To minimize the potential for suffering, beginning at 100 days of age, food pellets were placed on the cage floor, and hydrating gel (Napa Nectar, Lenderking, Millersville, MD, USA) was provided. Mice were also assessed daily and euthanized if unable to right themselves from supine within 30 s.

mRNA Quantification by RT-PCR

mRNA was isolated from brain tissue by using a microRNeasy kit (QIAGEN, Germantown, MD, USA), according to the manufacturer's instructions. RNA (10 ng) was transcribed with the High Capacity cDNA Reverse Transcription kit (Thermo Fisher Scientific, Waltham, MA, USA), and 3 μL cDNA was used in each qPCR reaction. The relative expression of GFAP (probe mm01253033-m1), CD68 (probe mm03047343-m1), and Gpnmb (probe mm01328587) was analyzed by the $2^{-\Delta\Delta Ct}$ method. Values were normalized to GapDH (probe mm99999915-g1) within each sample. Sample groups were normalized to the WT-UNT sample. qPCR was performed on a QuantStudio Flex 7 System with probe sets and universal master mix (Thermo Fisher Scientific, Waltham, MA, USA).

Rotarod Analysis

Mice were evaluated for motor coordination and endurance on an accelerating rotarod (Ugo Basile 47600; Stoelting Co., Wood Dale, IL, USA), starting when the animals were 84 days of age and repeated every 2 weeks. The assay consisted of placing the mice on a spindle rotating at 5 rpm, which was gradually increased to 40 rpm over 5 minutes. Each animal was subjected to four trials at each time point, and the time to fall (latency) was recorded. The first result on each assay day was discarded, and there was a 1 h rest period included between each trial.

Fluorescent TSPO-Ligand Imaging

One day prior to TSPO-ligand fluorescence imaging, mouse head fur (between the ears, nose-to-neck region) was removed by applying a thin layer of depilatory cream (Nair, Church & Dwight, Ewing, NJ, USA) to isoflurane anesthetized mouse. After 2–3 min, the cream and hair were removed by gently wiping the area several times with moistened gauze pads.

For these imaging studies, a near-infrared fluorescent (NIRF) translocator protein (TSPO) probe, VUIIS-1520 (Vanderbilt Center for Molecular Probes, Nashville, TN, USA), was used. This is similar to the TSPO-PET ligand, [^{18}F]VUIIS-1008[57,58] but harbors an infrared dye (LI-COR IRDye 800CW). The probe has an excitation maximum at 779 nm and emission maximum at 789 nm, a molar extinction coefficient of 27,920.15 L/mol/cm in PBS at room temperature, and a TSPO binding affinity IC_{50} of 9.83 nM, as measured in a C6 glioma cell lysate assay. The VUIIS-1520 was administered intravenously via tail vein at a dose of 0.15 mg/kg in 1% DMSO, with PBS as the vehicle. Fluorescence was imaged with the IVIS SpectrumCT *in vivo* imaging system (PerkinElmer, Hopkinton, MA, USA) at multiple time points (from 30 min to 4 weeks after the probe dose) in live mice, serum samples, and various tissue samples. A pseudo-color scheme generated by Living Imaging software (version 4.5.2; PerkinElmer) was used to visualize the numerical readout of the acquired fluorescence signal. To quantify fluorescence emission signal, identical regions of interest (ROIs) of each mouse head were imaged, and the imaging signal was quantitated as total radiant efficiency ([p/s]/[μW/cm^2]) for the indicated ROI. With the ROI kept constant in area and position for a study, these two units were proportional, and data could be normalized to fluorescence prior to the initiation of treatment for each animal. *Ex vivo* fluorescence imaging of isolated organs was performed immediately after euthanasia of the animals with CO_2. All dissected organs were placed on black paper, covered with a plastic sheet, and imaged at the same time point.

For statistical analysis of the TSPO imaging data, the EverStart V5 (SAS JMP, Cary, NC, USA) and SigmaStat (Systat Software Inc.,

San Jose, CA, USA) statistical software packages were used. For comparison of group means, a paired Wilcoxon test or unpaired Wilcoxon test was conducted. Two-tailed values of $p < 0.05$ were considered statistically significant.

Measurement of Brain Gliosis

Unstained sagittal sections of formalin-fixed, paraffin-embedded mouse brains were subjected to IHC, with a Bond-Max automated immunostainer (Leica Biosystems, Buffalo Grove, IL, USA) according to the manufacturer's recommended protocol for heat-induced epitope retrieval in EDTA buffer (pH 9.0) for 10 min. Goat polyclonal anti-mouse antibody (Gpnmb/osteoactivin; R&D Systems, Inc. Minneapolis, MN, USA) was used as the primary antibody (working concentration, 0.15625 μg/mL) and $F(ab')_2$ fragment rabbit anti-goat immunoglobulin G (IgG; Jackson ImmunoResearch Laboratories, West Grove, PA, USA) as the secondary antibody (working concentration, 2.6 μg/mL). As a negative control for the IHC assay, serial sections were also subjected to IHC, using goat IgG (Jackson ImmunoResearch Laboratories, West Grove, PA, USA) at the same working concentration as the primary antibody. Diaminobenzidine (DAB) was used as the chromogen for bright-field detection of the IHC reaction. IHC slides were qualitatively evaluated for specificity and sensitivity of immunostaining by a board-certified veterinary pathologist. Digital images were obtained at ×100 magnification via NIS-Elements microscope imaging software (Nikon Instruments, Melville, NY, USA). Images were then analyzed for percentage of Gpnmb-immunopositive areas, using the area quantitation algorithm of HALO image-analysis software (Indica Lab, Corrales, NM, USA).

Sphingolipid Quantification by MS Analysis

Quantitative analysis of sphingolipids was performed by liquid chromatography (LC) and high-resolution MS (LC/HR-MS) or LC-MS/MS, previously, as were the extraction and analysis of GL1.[23] Solvents were modified for ganglioside, GA2, and GL4 extraction and analysis. Briefly, an aliquot of tissue homogenate (5 μL for brain and 10 μL for the other tissues) was extracted with 1 mL of an organic solvent mixture consisting of equal volumes of acetonitrile and methanol. GM1, GM2, GM3, GL4, GA2, and LysoGM2 were separated on a Waters Acquity ultra-high-performance LC (UPLC) and Waters Cortecs hydrophilic-interaction LC (HILIC) column (2.7 μm; 2.1 × 100 mm) at room temperature. The gradient started with 100% mobile phase A (acetonitrile:water [95:5] in 5 mM ammonium acetate and 0.02% acetic acid) and ended after 3 min with 40% mobile phase B (methanol:water [1:1] in 5 mM ammonium acetate and 0.02% acetic acid). This was followed by a wash with 100% phase B and re-equilibration with 100% phase A. The total run time was 7.5 min, and the flow-rate was 0.6 mL/min. Eluent was analyzed with a Q Exactive Focus mass spectrometer (Thermo Fisher Scientific, Waltham, MA, USA) equipped with a heated electrospray ionization (HESI) source with the following parameters: sheath gas flow rate of 50, auxiliary gas flow rate of 10, sweep gas flow rate of 0, spray voltage of 3.5 kV, capillary temperature of 350°C, S-lens radiofrequency (RF) level of 90, and auxiliary gas heater temperature of 500°C. Data were collected in full MS positive mode, using the following parameters: resolution of 70,000; scan range of m/z 700–1,700, automatic gain control target of 3e6, and maximum injection time (IT) of 240 ms. Quantitation of different isoforms (with various acyl chain lengths and 2-hyroxylation) was achieved by MS1 extraction of ion chromatograms from positive scan using Skyline software (MacCoss Lab, University of Washington, Seattle, WA, USA).[59] GM1, GM2, GM3, GL4, and GA2 standards were purchased from Matreya (Pleasant Gap, PA, USA). LysoGM2 standard was purchased from TaKaRa (Kyoto, Japan).

tMSI Analysis

The MALDI matrices for negative ionization—1,5-diaminonaphthalene (DAN), 9-aminoacridine (9-AA), and ammonium formate—were from Sigma-Aldrich (St. Louis, MO, USA). Solvents, high-performance-LC (HPLC)-grade water, methanol, and ethanol, were from OmniSolve (McLean, VA, USA). Indium-tin-oxide (ITO)-coated slides were from HTX Technologies (Chapel Hill, NC, USA). 2-Methylbutane was from Thermo Fisher Scientific (Waltham, MA, USA). Tissue-Tek optimal cutting temperature (OCT) compound was from VWR (Radnor, PA).

Fresh brains were collected in plastic molds and frozen by floating the molds in a slurry bath of dry ice and 2-methylbutane. Different MALDI matrixes were tested to identify optimal ionization of targeted compounds, and DAN matrix was chosen for negative ion mode analysis. The TM-Sprayer (HTX Technologies, Chapel Hill, NC, USA) was used to deposit the matrices on ITO-coated slides. A solution of 5 mg/mL DAN in 70% methanol was sprayed at 75°C, using a double perpendicular raster in eight passes. Brains were attached to the chilled chuck with a drop of OCT compound, making sure that the OCT did not touch the targeted brain area or the cryostat blade. The brains were sectioned in sagittal slices of 10 μm at −20°C, using a cryostat (Leica Biosystems, Buffalo Grove, IL, USA). Organ sections were deposited on top of ITO-coated slides, which were covered in advance with DAN matrix.[60] Tissue sections subjected to MS analysis were pretreated with 50 mM ammonium formate aqueous solutions for 30 s, to enhance the signal of low-abundance glycolipids.[61] Image acquisition was performed in negative ion mode at 35 μm spatial resolution on brain sections from each experimental group, using the Autoflex (Bruker Daltonics, Billerica, MA, USA) MALDI-TOF/TOF mass spectrometer. Images were generated using FlexImaging (Bruker Daltonics) software and normalized using the root-mean-square algorithm. Tissue quantitation and statistical analyses were performed with SCiLS Lab software (Bruker Daltonics). Unless otherwise noted, all statistics were analyzed in GraphPad Prism 7.0 software (LaJolla, CA, USA).

SUPPLEMENTAL INFORMATION

Supplemental Information can be found online at https://doi.org/10.1016/j.ymthe.2019.05.018.

AUTHOR CONTRIBUTIONS

Conceptualization: J.M., S.H.C., and J.P.L.; Writing – Manuscript Draft: J.M. and S.H.C.; Experiment Performance: J.M., J.B.N., H.P.,

K.R., D.T., D.S.B., T.W., J.C., and C.S.; Analysis and Interpretation: J.M., J.B.N., D.S.B., C.S., B.W., and X.Y.

CONFLICTS OF INTEREST

All authors were shareholders of Sanofi, S.A., stock and/or employees of Sanofi at the time of the study.

ACKNOWLEDGMENTS

The authors would like to thank our colleagues Leah Curtin, Karen Norton, Megan Pike, and other members of the In Vivo Research Center for their assistance with animal studies. We would also like to acknowledge members of the Histology and Pathology departments for their expertise in processing the tissue samples, and Ray Gimi, Jin Zhao, Paul Konowicz, and Mike Reardon, members of the chemistry department, for the synthesis and purification of Genz-682452. We give special acknowledgment to Professor H. Charles Manning, Vanderbilt University Institute of Imaging Science, Nashville, TN, for supplying VUIIS-1520.

REFERENCES

1. Gravel, R.A., Kaback, M.M., Proia, R.L., Sandhoff, K., Suzuki, K., and Suzuki, K. (2014). The G_{M2} Gangliosidoses. In The Online Metabolic and Molecular Bases of Inherited Disease, D. Valle, A.L. Beaudet, B. Vogelstein, K.W. Kinzler, S.E. Antonarakis, and A. Ballabio, et al., eds. (McGraw-Hill Medical), https://ommbid.mhmedical.com/book.aspx?bookid=971.
2. Nestrasil, I., Ahmed, A., Utz, J.M., Rudser, K., Whitley, C.B., and Jarnes-Utz, J.R. (2018). Distinct progression patterns of brain disease in infantile and juvenile gangliosidoses: Volumetric quantitative MRI study. Mol. Genet. Metab. *123*, 97–104.
3. Jarnes Utz, J.R., Kim, S., King, K., Ziegler, R., Schema, L., Redtree, E.S., and Whitley, C.B. (2017). Infantile gangliosidoses: Mapping a timeline of clinical changes. Mol. Genet. Metab. *121*, 170–179.
4. Bradbury, A.M., Peterson, T.A., Gross, A.L., Wells, S.Z., McCurdy, V.J., Wolfe, K.G., Dennis, J.C., Brunson, B.L., Gray-Edwards, H., Randle, A.N., et al. (2017). AAV-mediated gene delivery attenuates neuroinflammation in feline Sandhoff disease. Neuroscience *340*, 117–125.
5. Niemir, N., Rouvière, L., Besse, A., Vanier, M.T., Dmytrus, J., Marais, T., Astord, S., Puech, J.P., Panasyuk, G., Cooper, J.D., et al. (2018). Intravenous administration of scAAV9-Hexb normalizes lifespan and prevents pathology in Sandhoff disease mice. Hum. Mol. Genet. *27*, 954–968.
6. Chiricozzi, E., Niemir, N., Aureli, M., Magini, A., Loberto, N., Prinetti, A., Bassi, R., Polchi, A., Emiliani, C., Caillaud, C., and Sonnino, S. (2014). Chaperone therapy for GM2 gangliosidosis: effects of pyrimethamine on β-hexosaminidase activity in Sandhoff fibroblasts. Mol. Neurobiol. *50*, 159–167.
7. Arthur, J.R., Lee, J.P., Snyder, E.Y., and Seyfried, T.N. (2012). Therapeutic effects of stem cells and substrate reduction in juvenile Sandhoff mice. Neurochem. Res. *37*, 1335–1343.
8. Norflus, F., Tifft, C.J., McDonald, M.P., Goldstein, G., Crawley, J.N., Hoffmann, A., Sandhoff, K., Suzuki, K., and Proia, R.L. (1998). Bone marrow transplantation prolongs life span and ameliorates neurologic manifestations in Sandhoff disease mice. J. Clin. Invest. *101*, 1881–1888.
9. Jeyakumar, M., Norflus, F., Tifft, C.J., Cortina-Borja, M., Butters, T.D., Proia, R.L., Perry, V.H., Dwek, R.A., and Platt, F.M. (2001). Enhanced survival in Sandhoff disease mice receiving a combination of substrate deprivation therapy and bone marrow transplantation. Blood *97*, 327–329.
10. Tsuji, D., Akeboshi, H., Matsuoka, K., Yasuoka, H., Miyasaki, E., Kasahara, Y., Kawashima, I., Chiba, Y., Jigami, Y., Taki, T., et al. (2011). Highly phosphomannosylated enzyme replacement therapy for GM2 gangliosidosis. Ann. Neurol. *69*, 691–701.
11. Kitakaze, K., Mizutani, Y., Sugiyama, E., Tasaki, C., Tsuji, D., Maita, N., Hirokawa, T., Asanuma, D., Kamiya, M., Sato, K., et al. (2016). Protease-resistant modified human β-hexosaminidase B ameliorates symptoms in GM2 gangliosidosis model. J. Clin. Invest. *126*, 1691–1703.
12. Andersson, U., Smith, D., Jeyakumar, M., Butters, T.D., Borja, M.C., Dwek, R.A., and Platt, F.M. (2004). Improved outcome of N-butyldeoxygalactonojirimycin-mediated substrate reduction therapy in a mouse model of Sandhoff disease. Neurobiol. Dis. *16*, 506–515.
13. Baek, R.C., Kasperzyk, J.L., Platt, F.M., and Seyfried, T.N. (2008). N-butyldeoxygalactonojirimycin reduces brain ganglioside and GM2 content in neonatal Sandhoff disease mice. Neurochem. Int. *52*, 1125–1133.
14. Ashe, K.M., Bangari, D., Li, L., Cabrera-Salazar, M.A., Bercury, S.D., Nietupski, J.B., Cooper, C.G., Aerts, J.M., Lee, E.R., Copeland, D.P., et al. (2011). Iminosugar-Based Inhibitors of Glucosylceramide Synthase Increase Brain Glycosphingolipids and Survival in a Mouse Model of Sandhoff Disease. PLoS One *6*, e21758.
15. Hocquemiller, M., Giersch, L., Audrain, M., Parker, S., and Cartier, N. (2016). Adeno-Associated Virus-Based Gene Therapy for CNS Diseases. Hum. Gene Ther. *27*, 478–496.
16. Saraiva, J., Nobre, R.J., and Pereira de Almeida, L. (2016). Gene therapy for the CNS using AAVs: The impact of systemic delivery by AAV9. J. Control. Release *241*, 94–109.
17. Henig, I., and Zuckerman, T. (2014). Hematopoietic stem cell transplantation-50 years of evolution and future perspectives. Rambam Maimonides Med. J. *5*, e0028.
18. Sands, M.S. (2014). A Hitchhiker's guide to the blood-brain barrier: in trans delivery of a therapeutic enzyme. Mol. Ther. *22*, 483–484.
19. Cox, T.M., Aerts, J.M., Andria, G., Beck, M., Belmatoug, N., Bembi, B., Chertkoff, R., Vom Dahl, S., Elstein, D., Erikson, A., et al.; Advisory Council to the European Working Group on Gaucher Disease (2003). The role of the iminosugar N-butyldeoxynojirimycin (miglustat) in the management of type I (non-neuronopathic) Gaucher disease: a position statement. J. Inherit. Metab. Dis. *26*, 513–526.
20. Smid, B.E., and Hollak, C. (2014). A systematic review on effectiveness and safety of eliglustat for type 1 Gaucher disease. Expert Opin. Orphan Drugs *2*, 523–529.
21. Jeyakumar, M., Butters, T.D., Cortina-Borja, M., Hunnam, V., Proia, R.L., Perry, V.H., Dwek, R.A., and Platt, F.M. (1999). Delayed symptom onset and increased life expectancy in Sandhoff disease mice treated with N-butyldeoxynojirimycin. Proc. Natl. Acad. Sci. USA *96*, 6388–6393.
22. Cabrera-Salazar, M.A., Deriso, M., Bercury, S.D., Li, L., Lydon, J.T., Weber, W., Pande, N., Cromwell, M.A., Copeland, D., Leonard, J., et al. (2012). Systemic delivery of a glucosylceramide synthase inhibitor reduces CNS substrates and increases lifespan in a mouse model of type 2 Gaucher disease. PLoS ONE *7*, e43310.
23. Marshall, J., Sun, Y., Bangari, D.S., Budman, E., Park, H., Nietupski, J.B., Allaire, A., Cromwell, M.A., Wang, B., Grabowski, G.A., et al. (2016). CNS-accessible Inhibitor of Glucosylceramide Synthase for Substrate Reduction Therapy of Neuronopathic Gaucher Disease. Mol. Ther. *24*, 1019–1029.
24. Ashe, K.M., Budman, E., Bangari, D.S., Siegel, C.S., Nietupski, J.B., Wang, B., Desnick, R.J., Scheule, R.K., Leonard, J.P., Cheng, S.H., and Marshall, J. (2015). Efficacy of enzyme and substrate reduction therapy with a novel antagonist of glucosylceramide synthase for Fabry disease. Mol. Med. *21*, 389–399.
25. Sango, K., Yamanaka, S., Hoffmann, A., Okuda, Y., Grinberg, A., Westphal, H., McDonald, M.P., Crawley, J.N., Sandhoff, K., Suzuki, K., and Proia, R.L. (1995). Mouse models of Tay-Sachs and Sandhoff diseases differ in neurologic phenotype and ganglioside metabolism. Nat. Genet. *11*, 170–176.
26. Beckers, L., Ory, D., Geric, I., Declercq, L., Koole, M., Kassiou, M., Bormans, G., and Baes, M. (2018). Increased Expression of Translocator Protein (TSPO) Marks Pro-inflammatory Microglia but Does Not Predict Neurodegeneration. Mol. Imaging Biol. *20*, 94–102.
27. Coutinho, M.F., Santos, J.I., and Alves, S. (2016). Less Is More: Substrate Reduction Therapy for Lysosomal Storage Disorders. Int. J. Mol. Sci. *17*, E1065.
28. Cox, T.M., Drelichman, G., Cravo, R., Balwani, M., Burrow, T.A., Martins, A.M., Lukina, E., Rosenbloom, B., Goker-Alpan, O., Watman, N., et al. (2017). Eliglustat maintains long-term clinical stability in patients with Gaucher disease type 1 stabilized on enzyme therapy. Blood *129*, 2375–2383.
29. Mistry, P.K., Lukina, E., Ben Turkia, H., Shankar, S.P., Baris, H., Ghosn, M., Mehta, A., Packman, S., Pastores, G., Petakov, M., et al. (2017). Outcomes after 18 months of

eliglustat therapy in treatment-naïve adults with Gaucher disease type 1: The phase 3 ENGAGE trial. Am. J. Hematol. *92*, 1170–1176.

30. Liu, Y., Wada, R., Kawai, H., Sango, K., Deng, C., Tai, T., McDonald, M.P., Araujo, K., Crawley, J.N., Bierfreund, U., et al. (1999). A genetic model of substrate deprivation therapy for a glycosphingolipid storage disorder. J. Clin. Invest. *103*, 497–505.
31. Seyrantepe, V., Demir, S.A., Timur, Z.K., Von Gerichten, J., Marsching, C., Erdemli, E., Oztas, E., Takahashi, K., Yamaguchi, K., Ates, N., et al. (2018). Murine Sialidase Neu3 facilitates GM2 degradation and bypass in mouse model of Tay-Sachs disease. Exp. Neurol. *299*, 26–41.
32. Seyrantepe, V., Lema, P., Caqueret, A., Dridi, L., Bel Hadj, S., Carpentier, S., Boucher, F., Levade, T., Carmant, L., Gravel, R.A., et al. (2010). Mice doubly-deficient in lysosomal hexosaminidase A and neuraminidase 4 show epileptic crises and rapid neuronal loss. PLoS Genet. *6*, e1001118.
33. Yamanaka, S., Johnson, M.D., Grinberg, A., Westphal, H., Crawley, J.N., Taniike, M., Suzuki, K., and Proia, R.L. (1994). Targeted disruption of the Hexa gene results in mice with biochemical and pathologic features of Tay-Sachs disease. Proc. Natl. Acad. Sci. USA *91*, 9975–9979.
34. Dekker, N., van Dussen, L., Hollak, C.E.M., Overkleeft, H., Scheij, S., Ghauharali, K., van Breemen, M.J., Ferraz, M.J., Groener, J.E., Maas, M., et al. (2011). Elevated plasma glucosylsphingosine in Gaucher disease: relation to phenotype, storage cell markers, and therapeutic response. Blood *118*, e118–e127.
35. Escolar, M.L., Kiely, B.T., Shawgo, E., Hong, X., Gelb, M.H., Orsini, J.J., Matern, D., and Poe, M.D. (2017). Psychosine, a marker of Krabbe phenotype and treatment effect. Mol. Genet. Metab. *121*, 271–278.
36. Nowak, A., Mechtler, T.P., Hornemann, T., Gawinecka, J., Theswet, E., Hilz, M.J., and Kasper, D.C. (2018). Genotype, phenotype and disease severity reflected by serum LysoGb3 levels in patients with Fabry disease. Mol. Genet. Metab. *23*, 148–153.
37. Nowak, A., Mechtler, T., Kasper, D.C., and Desnick, R.J. (2017). Correlation of Lyso-Gb3 levels in dried blood spots and sera from patients with classic and Later-Onset Fabry disease. Mol. Genet. Metab. *121*, 320–324.
38. Lloyd-Evans, E., Pelled, D., Riebeling, C., and Futerman, A.H. (2003). Lyso-glycosphingolipids mobilize calcium from brain microsomes via multiple mechanisms. Biochem. J. *375*, 561–565.
39. Yamaguchi, Y., Sasagasako, N., Goto, I., and Kobayashi, T. (1994). The synthetic pathway for glucosylsphingosine in cultured fibroblasts. J. Biochem. *116*, 704–710.
40. Kodama, T., Togawa, T., Tsukimura, T., Kawashima, I., Matsuoka, K., Kitakaze, K., Tsuji, D., Itoh, K., Ishida, Y., Suzuki, M., et al. (2011). Lyso-GM2 Ganglioside: A Possible Biomarker of Tay-Sachs Disease and Sandhoff Disease. PLoS One *6*, e29074.
41. Neuenhofer, S., Conzelmann, E., Schwarzmann, G., Egge, H., and Sandhoff, K. (1986). Occurrence of lysoganglioside lyso-GM2 (II3-Neu5Ac-gangliotriaosylsphingosine) in GM2 gangliosidosis brain. Biol. Chem. Hoppe Seyler *367*, 241–244.
42. Wada, R., Tifft, C.J., and Proia, R.L. (2000). Microglial activation precedes acute neurodegeneration in Sandhoff disease and is suppressed by bone marrow transplantation. Proc. Natl. Acad. Sci. USA *97*, 10954–10959.
43. Jeyakumar, M., Thomas, R., Elliot-Smith, E., Smith, D.A., van der Spoel, A.C., d'Azzo, A., Perry, V.H., Butters, T.D., Dwek, R.A., and Platt, F.M. (2003). Central nervous system inflammation is a hallmark of pathogenesis in mouse models of GM1 and GM2 gangliosidosis. Brain *126*, 974–987.
44. Wu, Y.-P., and Proia, R.L. (2004). Deletion of macrophage-inflammatory protein 1 alpha retards neurodegeneration in Sandhoff disease mice. Proc. Natl. Acad. Sci. USA *101*, 8425–8430.
45. Tsuji, D., Kuroki, A., Ishibashi, Y., Itakura, T., Kuwahara, J., Yamanaka, S., and Itoh, K. (2005). Specific induction of macrophage inflammatory protein 1-alpha in glial cells of Sandhoff disease model mice associated with accumulation of N-acetylhexosaminyl glycoconjugates. J. Neurochem. *92*, 1497–1507.
46. Tanaka, H., Shimazawa, M., Kimura, M., Takata, M., Tsuruma, K., Yamada, M., Takahashi, H., Hozumi, I., Niwa, J., Iguchi, Y., et al. (2012). The potential of GPNMB as novel neuroprotective factor in amyotrophic lateral sclerosis. Sci. Rep. *2*, 573.
47. Zigdon, H., Savidor, A., Levin, Y., Meshcheriakova, A., Schiffmann, R., and Futerman, A.H. (2015). Identification of a biomarker in cerebrospinal fluid for neuronopathic forms of Gaucher disease. PLoS ONE *10*, e0120194.
48. Vitner, E.B., Farfel-Becker, T., Ferreira, N.S., Leshkowitz, D., Sharma, P., Lang, K.S., and Futerman, A.H. (2016). Induction of the type I interferon response in neurological forms of Gaucher disease. J. Neuroinflammation *13*, 104.
49. Hillmer, A.T., Holden, D., Fowles, K., Nabulsi, N., West, B.L., Carson, R.E., and Cosgrove, K.P. (2017). Microglial depletion and activation: A [^{11}C]PBR28 PET study in nonhuman primates. EJNMMI Res. *7*, 59.
50. Zürcher, N.R., Loggia, M.L., Lawson, R., Chonde, D.B., Izquierdo-Garcia, D., Yasek, J.E., Akeju, O., Catana, C., Rosen, B.R., Cudkowicz, M.E., et al. (2015). Increased in vivo glial activation in patients with amyotrophic lateral sclerosis: assessed with [(11)C]-PBR28. Neuroimage Clin. *7*, 409–414.
51. Alam, M.M., Lee, J., and Lee, S.-Y. (2017). Recent Progress in the Development of TSPO PET Ligands for Neuroinflammation Imaging in Neurological Diseases. Nucl. Med. Mol. Imaging *51*, 283–296.
52. Loth, M.K., Choi, J., McGlothan, J.L., Pletnikov, M.V., Pomper, M.G., and Guilarte, T.R. (2016). TSPO in a murine model of Sandhoff disease: presymptomatic marker of neurodegeneration and disease pathophysiology. Neurobiol. Dis. *85*, 174–186.
53. Arbo, B.D., Benetti, F., Garcia-Segura, L.M., and Ribeiro, M.F. (2015). Therapeutic actions of translocator protein (18 kDa) ligands in experimental models of psychiatric disorders and neurodegenerative diseases. J. Steroid Biochem. Mol. Biol. *154*, 68–74.
54. Bembi, B., Marchetti, F., Guerci, V.I., Ciana, G., Addobbati, R., Grasso, D., Barone, R., Cariati, R., Fernandez-Guillen, L., Butters, T., and Pittis, M.G. (2006). Substrate reduction therapy in the infantile form of Tay-Sachs disease. Neurology *66*, 278–280.
55. Bembi, B., Ciana, G., and Zanatta, M. (2005). Cerebrospinal fluid infusion of alglucerase in the treatment of acute neuronopathic Gaucher's disease. Pediatr. Res. *38*, 425.
56. Gornati, R., Berra, B., Montorfano, G., Martini, C., Ciana, G., Ferrari, P., Romano, M., and Bembi, B. (2002). Glycolipid analysis of different tissues and cerebrospinal fluid in type II Gaucher disease. J. Inherit. Metab. Dis. *25*, 47–55.
57. Tang, D., Nickels, M.L., Tantawy, M.N., Buck, J.R., and Manning, H.C. (2014). Preclinical imaging evaluation of novel TSPO-PET ligand 2-(5,7-Diethyl-2-(4-(2-[(18)F]fluoroethoxy)phenyl)pyrazolo[1,5-a]pyrimidin-3-yl)-N,N-diethylacetamide ([(18)F]VUIIS1008) in glioma. Mol. Imaging Biol. *16*, 813–820.
58. Pulagam, K.R., Colás, L., Padro, D., Plaza-García, S., Gómez-Vallejo, V., Higuchi, M., Llop, J., and Martín, A. (2017). Evaluation of the novel TSPO radiotracer [^{18}F] VUIIS1008 in a preclinical model of cerebral ischemia in rats. EJNMMI Res. *7*, 93.
59. Schilling, B., Rardin, M.J., MacLean, B.X., Zawadzka, A.M., Frewen, B.E., Cusack, M.P., Sorensen, D.J., Bereman, M.S., Jing, E., Wu, C.C., et al. (2012). Platform-independent and label-free quantitation of proteomic data using MS1 extracted ion chromatograms in skyline: application to protein acetylation and phosphorylation. Mol. Cell. Proteomics *11*, 202–214.
60. Yang, J., and Caprioli, R.M. (2013). Matrix precoated targets for direct lipid analysis and imaging of tissue. Anal. Chem. *85*, 2907–2912.
61. Angel, P.M., Spraggins, J.M., Baldwin, H.S., and Caprioli, R. (2012). Enhanced sensitivity for high spatial resolution lipid analysis by negative ion mode matrix assisted laser desorption ionization imaging mass spectrometry. Anal. Chem. *84*, 1557–1564.